Measurement of the Elastic Magnetic Form Factor of ³He at High Momentum Transfer

I. Nakagawa,[2,*] J. Shaw,[1] S. Churchwell,[1,†] X. Jiang,[1,‡] B. Asavapibhop,[1] M. C. Berisso,[1,§] P. E. Bosted,[1]
K. Burchesky,[1] F. Casagrande,[3] A. Cichocki,[4] R. S. Hicks,[1] A. Hotta,[1] T. Kobayashi,[5] R. A. Miskimen,[1]
G. A. Peterson,[1] S. E. Rock,[1] T. Suda,[2,‖] T. Tamae,[2] W. Turchinetz,[3] and K. Wang[4]

[1]*Department of Physics, University of Massachusetts, Amherst, Massachusetts, 01003*
[2]*Laboratory of Nuclear Science, Tohoku University, Sendai 982-0826, Japan*
[3]*MIT-Bates Linear Accelerator Center, Middleton, Massachusetts 01949*
[4]*Department of Physics, University of Virginia, Charlottesville, Virginia 22901*
[5]*College of Radiology, Teikyo University, Tokyo 173-8605, Japan*
(Received 29 August 2000; revised manuscript received 19 March 2001)

New electron scattering measurements have been made that extend data on the ³He elastic magnetic form factor up to $Q^2 = 42.6$ fm^{-2}. These new data test theoretical conjectures regarding non-nucleonic effects in the three-body system. The very small cross sections, as low as 10^{-40} cm²/sr, required the use of a high-pressure cryogenic gas target and a detector system with excellent background rejection capability. No existing theoretical calculation satisfactorily accounts for all the available data.

Because their ground-state wave functions may be calculated exactly for a given nucleon-nucleon potential, three-body nuclei strongly test theoretical conjectures regarding meson-exchange currents, Δ isobars, and other non-nucleonic degrees of freedom. Because of a destructive interference between S- and D-state components of the ground-state wave function, the magnetic form factor $F_M(Q^2)$ of ³He is particularly sensitive to non-nucleonic effects. Calculations without non-nucleonic effects predict a diffraction minimum in $F_M(Q^2)$ near four-momentum transfer-squared $Q^2 = 8$ fm^{-2}, in striking disagreement with experimental results [1–8] that indicate the minimum lies in the range $Q^2 = 17–19$ fm^{-2}. This dramatic upward shift in Q^2 is qualitatively explained by calculations [9–11] that include meson-exchange and Δ-isobar currents, making ³He one of the very few cases in which non-nucleonic effects are manifested so unambiguously. Notwithstanding this improvement, the diffraction minimum is still predicted at a Q^2 that is too low. Moreover, in the $Q^2 > 32$ fm^{-2} region, where no data exist, the calculations diverge by orders of magnitude, primarily due to their varied handling of non-nucleonic effects [12].

We present here a new measurement of the ³He magnetic form factor that extends data up to $Q^2 = 42.6$ fm^{-2}. At Q^2 values of this magnitude, theoretical treatments based solely on nucleon and meson degrees of freedom will be severely tested, and the consequences of the underlying quark-gluon dynamics may appear. Measurements were also made at $Q^2 = 18.8$ and 21.8 fm^{-2} in order to better determine the position of the diffraction minimum that so strongly constrains theoretical interpretations.

The experiment was carried out at the MIT-Bates Linear Accelerator Center using a 1% duty-factor electron beam and a high-density cryogenic ³He gas target. Scattered electrons were momentum analyzed by a 2.54 m bending-radius magnetic spectrometer, which was set to a scattering angle of $\theta = 160°$ in order to suppress charge scattering.

About 4000 STP liters of ³He were cooled to 23 K and pressurized to 50 atm, resulting in a 65 ± 2 mg/cm³ gas density [13]. The gas was circulated at 3 m/s through an aluminum target cell followed by a heat exchanger that removed the heat deposited by the beam. The cell was cylindrical, 5.1 cm in diameter, 19.6 cm long, and was oriented with its axis parallel to the beam. It had 0.56-mm-thick side walls and 0.81-mm-thick round end caps [13]. In order to mitigate variations in the gas density due to beam heating, the gas flow was highly turbulent, an enlarged beam spot was used, and the beam current was held constant at 19 ± 1 μA. A slit was placed between the cell and the spectrometer so that electrons scattered from the end caps and a gas flow guide inside the cell did not enter the spectrometer. This slit, together with a collimator located at the entrance of the spectrometer, defined the acceptance solid angle of 3.4 μsr averaged over the 8.7 cm target length seen by the spectrometer. For the above conditions, the corresponding luminosity was 1.4×10^{37} cm^{-2} s^{-1}.

The spectrometer detector system consisted of two layers of vertical drift chambers for tracking, a gas Čerenkov detector and a lead-glass shower counter for particle identification, and three layers of plastic scintillators for triggering and timing [14]. The Čerenkov detector was filled with isobutane at atmospheric pressure, and had a detection threshold of 10 MeV for electrons, but $\geq$2000 MeV for muons and pions. The shower counter consisted of two rows of lead-glass blocks having a total thickness of 12 radiation lengths. In order to check the uniformity of the detection system response as a function of the interaction point within the target, an 11.3-cm-long carbon target inclined at 45° with respect to the beam direction was moved vertically through the beam. Within the experimental uncertainties, the detection system response was constant [13].

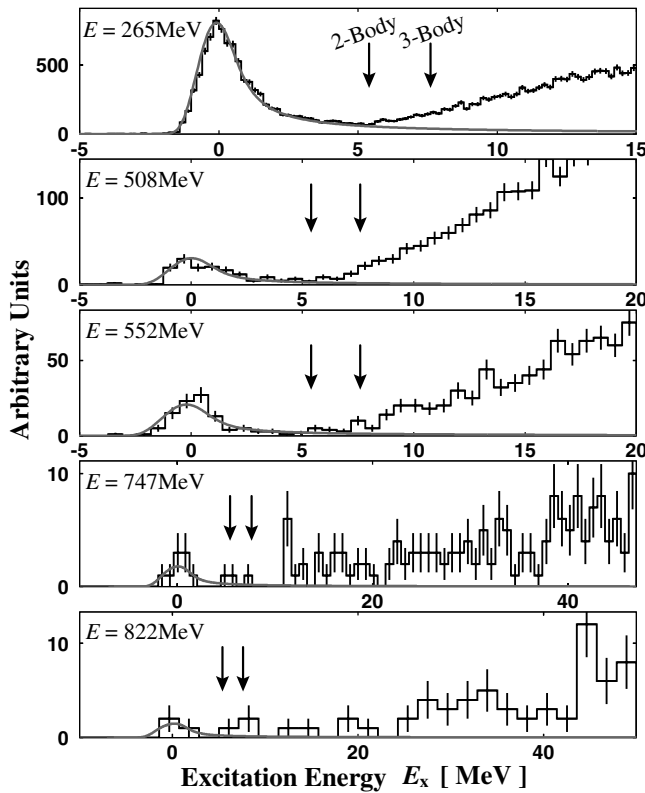Figure 1 shows the excitation energy spectra measured for ³He at five different incident energies. At the highest

FIG. 1. Background-corrected spectra measured for ^{3}He, showing the clear separation of the elastic peaks from the two-body (5.4 MeV) and three-body (7.6 MeV) breakup thresholds.

beam energy of 822 MeV, only three elastic counts were observed in four days of continuous measurement. The absence of counts in the kinematically disallowed $E_x < 0$ region demonstrates the high quality of the background rejection, especially in such a single-arm measurement. The elastic peaks are seen to be cleanly separated from the two-body breakup threshold at $E_x = 5.4$ MeV, and the peak shapes are well reproduced by calculations that include external and internal bremsstrahlung, and ionization in the ^{3}He gas and the target cell materials [15]. The convolution of these energy-loss processes in the calculation was simplified by using a near-peak approximation [16]. The long target length was also taken into account by simulating various scattering vertices along the beam axis. Based on these calculations, the multiplicative factors needed to correct the data up to the two-body threshold ranged from 1.27 to 1.40 depending on the beam energy.

In order to check the overall detection efficiency, the elastic ^{3}He cross section was measured at $Q^2 = 5.75$ fm^{-2}, a momentum transfer at which this cross section is known to 10% [1,3,4,6,8]. Using the same target system, we also measured the purely charge scattering cross section of ^{4}He at $Q^2 = 4.36$ fm^{-2} which has previously been determined to 3% [3,5,17]. Both measurements agree with previous data.

For the spin-$\frac{1}{2}$ ^{3}He nucleus the elastic cross section is related to the magnetic $F_M(Q^2)$ and charge $F_C(Q^2)$ form factors through the Rosenbluth formula:

$$\frac{d\sigma}{d\Omega} = \frac{\sigma_M}{1 + 2E\sin^2(\theta/2)/M} \left\{ \frac{Z^2|F_C(Q^2)|^2}{1 + \tau} + \tau\left(\frac{\mu M}{M_N}\right)^2 \right.$$
$$\times \left[\frac{1}{1 + \tau} + 2\tan^2\frac{\theta}{2} \right]$$
$$\left. \times |F_M(Q^2)|^2 \right\},$$

where E is the incident electron energy, Z, M, and μ are the charge, mass, and magnetic moment of the target nucleus, respectively, M_N is the nucleon mass, σ_M is the Mott cross section, and $\tau = Q^2/4M^2$. Charge contributions were assessed from a sum-of-Gaussian fit to the published results [8,18] shown in Fig. 2(a), permitting the magnetic form factor to be isolated. For the purpose of making more direct comparisons with theoretical predictions, the magnetic and charge form factors were then separately corrected for Coulomb distortion using a phase-shift analysis. The measured cross section, the calculated contribution of the charge form factor, and the corresponding corrected magnetic form factors are listed in Table I. The total systematic error, estimated to be 6.8%, was primarily due to uncertainties in the gas density and radiative corrections.

Figure 2(b) shows our new results and previous data [1–8]. The datum at $Q^2 = 5.75$ fm^{-2} agrees with previous measurements within the experimental uncertainty. The new data points at $Q^2 = 18.8$ and 21.8 fm^{-2} are consistent with previous data, strengthening the conclusion that the first diffraction minimum lies close to $Q^2 = 18$ fm^{-2}. The large error in the data point at 18.8 fm^{-2} results from the small contribution of magnetic scattering at $\theta = 160°$. Although charge scattering is greatly suppressed at this angle, it is still 6 times larger than magnetic scattering at this momentum transfer. The new data points at $Q^2 = 36.3$ and 42.6 fm^{-2} lie in a previously unexplored momentum transfer region. These data suggest a steep decline in the form factor, much steeper than would be predicted by extrapolating the previous Saclay results.

The calculations presented in Fig. 2 are by Hadjimichael et al. [9], Marcucci et al. [10], and Strueve et al. [11]. Hadjimichael et al. used the three-body wave functions obtained by solving the Faddeev equations with the Sprung–de Tourreil nucleon-nucleon interaction. Intermediate Δ-isobar components, excited by a three-body interaction represented by two-pion exchange, were also incorporated. Marcucci et al. used the Argonne two-nucleon v_{18} (AV18) interaction and the Urbana IX three-nucleon force. Two-body exchange currents were constructed whose leading terms were consistent with the AV18 interaction. Similar calculations using the AV18 interaction successfully account for both the charge and magnetic form factors of ^{3}H [10], as well as the form
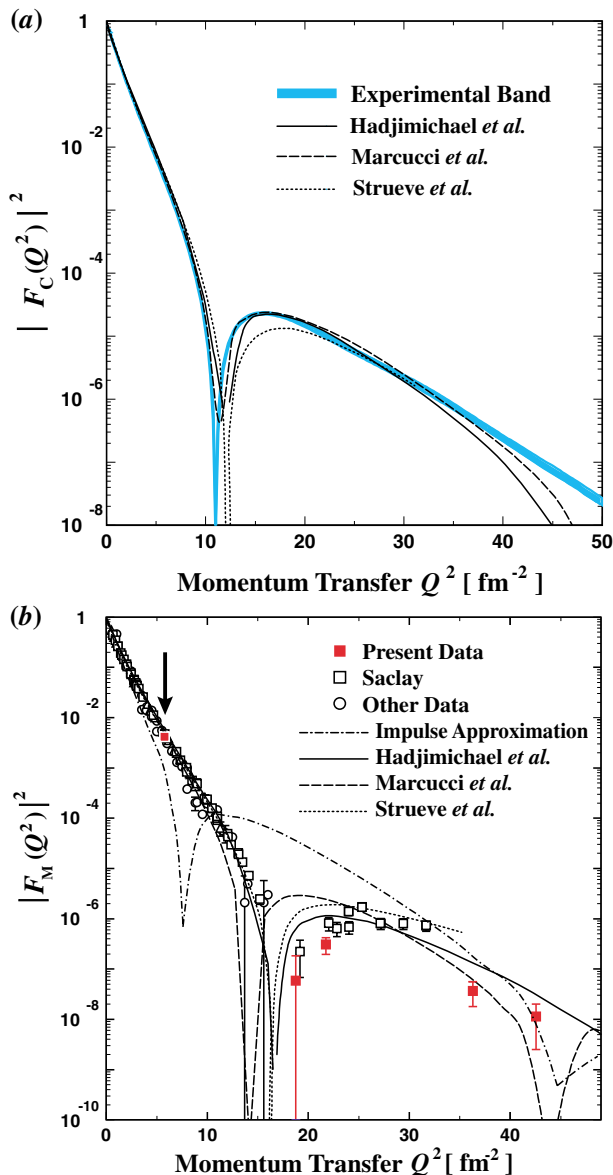
FIG. 2 (color). (a) Calculated form factors for elastic charge scattering from ^{3}He and comparison to sum-of-Gaussian fits [8,18] to experimental values. (b) Elastic magnetic form factor of ^{3}He. The Saclay data are from Refs. [7,8]; other data are from Refs. [1–6]. The arrow indicates the present measurement at $Q^2 = 5.75$ fm^{-2}. The impulse approximation curve is from Ref. [9].

factors of the deuteron up to $Q^2 = 50$ fm^{-2} [19]. In a third calculation, Strueve et al. used the Paris potential, modified by phenomenologically subtracting Δ processes. Those processes are included with two-body transition potentials due to π and ρ exchanges that are explicitly treated. The Δ excitations yield an important part of the three-nucleon interaction.

Of course, any satisfactory theoretical model should simultaneously describe both the charge and the magnetic form factors of ^{3}He. As indicated in Fig. 2(b), striking differences are observed between the various predictions

for the magnetic form factors in the vicinity of the first diffraction minimum and at high Q^2. All calculations place the diffraction minimum at a Q^2 that is too low, with the disagreement being largest in the calculations of Marcucci et al., who have elsewhere successfully accounted for diffraction minima in other $A = 3$, as well as $A = 2$, form factors. Although Strueve et al. provide a better account of the first diffraction minimum of ^{3}He, they noticeably underestimate the charge form factor in this same Q^2 region.

At higher Q^2 Strueve et al. obtain dominant meson-exchange and Δ terms, resulting in a predicted form factor that exceeds our highest Q^2 points by more than 1 order of magnitude. Remarkably different are the predictions of Marcucci et al. in which it is the basic one-nucleon term that provides the leading contribution at high Q^2. As a result, a second diffraction minimum is predicted at about 43 fm^{-2}. Further discussions of the differences between these theories can be found in Ref. [10]. The calculations of Hadjimichael et al. are in reasonable agreement with the experimental results for the magnetic form factor of ^{3}He; however, their calculation is less successful for the isovector $T = 1$ charge form factor at higher Q^2 [8]. In short, no existing theoretical treatments provide a satisfactory description of available data.

Significant relativistic effects may be expected in the large Q^2 region accessed by this experiment. Indeed, at these Q^2 values, sizeable relativistic components were obtained in realistic calculations for the deuteron, particularly in the magnetic form factor [20]. Relativistic bound-state wave functions derived for three-nucleon systems are notable for their precise prediction of the triton binding energy [21]. The inclusion of leading-order relativistic corrections also improves predictions for the three-nucleon form factors [11]; however, for these, no fully relativistic treatment has been made. The experimental results presented here should encourage such calculations.

For our results at the largest Q^2 values, where the characteristic distance scale is less than 1 fm, the relevance of the traditional nucleon-meson representation may be questioned. Indeed, scaling phenomena indicative of sub-nucleon structure were suggested [22] to set in at $Q^2 > 50$ fm^{-2} for the charge form factor of ^{3}He. Although our measurements do not extend to this Q^2 threshold, the gradual transition to quark-gluon dynamics may be reflected in our results. Exploratory attempts [23] to model this transition provide good fits to data in our Q^2 range.

In summary, the experimental results presented here provide new information on the ^{3}He elastic magnetic form factor at large Q^2 values, particularly above $Q^2 = 32$ fm^{-2}. Our measurements at $Q^2 = 18.8$ and 21.8 fm^{-2} strengthen the conclusion that the first diffraction minimum is located near $Q^2 = 18$ fm^{-2}, higher than the position predicted by current theories. In addition, an apparent sharp decrease observed in the form factor near $Q^2 = 35$ fm^{-2} may signal the existence of a second

TABLE I. Measured total cross sections, calculated charge contributions, and values extracted for the ^{3}He magnetic form factor. Listed uncertainties include statistical and systematic errors. Q^2 is calculated by taking into account the energy loss in the target and averaged over the acceptance.

E [MeV]	Q^2 [fm^{-2}]	$d\sigma/d\Omega$ [nb/sr]	charge [%]	$|F_M(Q^2)|^2$
265	5.75	$(1.81 \pm 0.12) \times 10^{-1}$	14	$(4.31 \pm 0.34) \times 10^{-3}$
508	18.8	$(3.55 \pm 0.37) \times 10^{-5}$	86	$(5.88 \pm 12.6) \times 10^{-8}$
552	21.8	$(2.49 \pm 0.30) \times 10^{-5}$	60	$(3.08 \pm 1.10) \times 10^{-7}$
747	36.3	$(1.16 \pm 0.39) \times 10^{-6}$	33	$(3.67 \pm 1.88) \times 10^{-8}$
822	42.6	$(2.84 \pm 1.65) \times 10^{-7}$	25	$(1.13 \pm 0.88) \times 10^{-8}$

diffraction minimum in the vicinity of $Q^2 = 40$ fm^{-2}. Future measurements planned at Jefferson Laboratory [24] should resolve this possibility.

New high-Q^2 results are also needed on the elastic form factors of tritium. At present, no existing theory simultaneously accounts for all of the experimental results on three-nucleon form factors, suggesting the need for improvements in non-nucleonic effects, relativistic treatments, and perhaps the inclusion of quark-gluon dynamics. The availability of comprehensive data on both the ^{3}He and ^{3}H form factors would permit a clean separation of isoscalar and isovector terms.

*Present address: Laboratory for Nuclear Science, MIT, Cambridge, Massachusetts 02139.
†Present address: Duke University, Durham, North Carolina 27708.
‡Present address: Rutgers, The State University of New Jersey, Piscataway, New Jersey 08855.
§Present address: Shasta College, Redding, California 96003.
‖Present address: The Institute of Physical and Chemical Research, Wako 351-0198, Japan.

[1] H. Collard et al., Phys. Rev. 138, B57 (1965).
[2] M. Bernheim et al., Lett. Nuovo Cimento 5, 431 (1972).
[3] J. S. McCarthy et al., Phys. Rev. C 15, 1396 (1977).
[4] P. C. Dunn et al., Phys. Rev. C 27, 71 (1983).
[5] C. R. Ottermann et al. Nucl. Phys. A436, 688 (1985).
[6] D. H. Beck et al., Phys. Rev. Lett. 59, 1537 (1987).
[7] J. M. Cavedon et al., Phys. Rev. Lett. 49, 986 (1982).
[8] A. Amroun et al., Phys. Rev. Lett. 69, 253 (1992); ibid., Nucl. Phys. A579, 596 (1994). A factor $1/\eta$ is a typographical error in formula (3) of the latter reference; S. K. Platchkov (private communication).
[9] E. Hadjimichael, B. Goulard, and R. Bornais, Phys. Rev. C 27, 831 (1983).
[10] L. E. Marcucci, D. O. Riska, and R. Schiavilla, Phys. Rev. C 58, 3069 (1998).
[11] W. Strueve, Ch. Hajduk, P. U. Sauer, and W. Theis, Nucl. Phys. A465, 651 (1987); H. Henning, P. U. Sauer, and W. Theis, Nucl. Phys. A537, 367 (1992)..
[12] J. Carlson and R. Schiavilla, Rev. Mod. Phys. 70, 743 (1998).
[13] I. Nakagawa, Ph. D. thesis, Tohoku University, 1999.
[14] X. Jiang, Ph. D. thesis, University of Massachusetts, 1998.
[15] L. W. Mo and Y. S. Tsai, Rev. Mod. Phys. 41, 205 (1969); Y. S. Tsai, Phys. Rev. 122, 1898 (1961).
[16] W. M. Schmitt et al., Phys. Rev. C 56, 1687 (1997).
[17] R. F. Frosch et al., Phys. Rev. 160, 874 (1967).
[18] R. G. Arnold et al., Phys. Rev. Lett. 40, 1429 (1978).
[19] R. B. Wiringa, V. G. J. Stoks, and R. Schiavilla, Phys. Rev. C 51, 38 (1995).
[20] J. W. Van Orden et al., Phys. Rev. Lett. 75, 4369 (1995).
[21] F. Gross, in Proceedings of the 2nd Workshop on Electronuclear Physics with Internal Targets and the BLAST Detector, Cambridge, 1998 (World Scientific, Singapore, 1999), p. 54.
[22] B. T. Chertok, Phys. Rev. Lett. 41, 1155 (1978).
[23] M. A. Maize and Y. E. Kim, Phys. Rev. C 35, 1060 (1987); H.-W. Ma and L. S. Kisslinger, Nucl. Phys. A531, 493 (1991).
[24] G. G. Petratos et al., JLab Report No. E00-118.